Adsorption of Organophosphates into Microporous and Mesoporous NaX Zeolites and Subsequent Chemistry
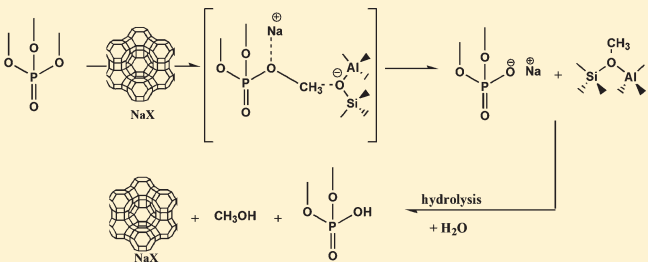
Qingguo Meng,*,[†] David C. Doetschman,[†] Apostolos K. Rizos,[‡] Min-Hong Lee,[†] Jürgen T. Schulte,[†] Apostolos Spyros,[‡] and Charles W. Kanyi[†]

[†]Department of Chemistry, Binghamton University, State University of New York, Vestal Parkway East, Binghamton, New York 13902-6000, United States

[‡]Department of Chemistry, University of Crete, Post Office Box 2208, 71003 Heraklion, Greece.

Ⓢ *Supporting Information*

ABSTRACT: Due to the neurotoxicity of organophosphate (OP) pesticides and nerve agents synthesized as military or terror agents, their safe destruction and disposal is of considerable current importance. A representative OP, trimethyl phosphate (TMP), was adsorbed onto NaX zeolite, two mesoporous modifications, and a low-silica X zeolite. The nucleophilic chemical reactions of TMP with the zeolites were investigated by solid-state ^{13}C and ^{31}P nuclear magnetic resonance (NMR) and the solvent extracts by ^1H, ^{13}C, and ^{31}P NMR. Nucleophilic substitution and subsequent hydrolysis reaction schemes are proposed. All of the zeolites have similar TMP decomposition yields, supporting the hypothesis that slow or incomplete diffusion of TMP in the microporous zeolite regions limits TMP decomposition.

1. INTRODUCTION

Organophosphates (OPs) refer broadly to a group of organic phosphorus(V) compounds that include neurotoxic pesticides or nerve agents, for both of which the salient property is the ability to bind to acetylcholinesterase (AChE), thereby disrupting nervous impulses and inhibiting the normal functions of nerve cells.[1] Exploring efficient ways to decontaminate OPs, with minimal environmental impact, has become a global necessity.[2] To date, numerous ways to degrade the OPs have been reported, such as enzymatic biodegradation,[3] electrochemical,[4] catalytic oxidation,[5] atmospheric pressure plasma,[6] and photolytic[7] methods. But hydrolysis methods on solid hosts have been widely applied, such as on fabrics,[8] TiO_2,[9] MgO,[10] nanometer-sized Al_2O_3,[11,12] ZnO,[13] Au/TiO_2,[14] activated carbons,[15] polymers,[16] mesoporous silica, etc.[17]

The most recent interests have been in the adsorption and hydrolysis of OPs in clay,[18] soil components,[19] and zeolites.[20] For example, VX nerve agent (*o*-ethyl *S*-[2-(diisopropylamino)ethyl] methylphosphonothioate) was reported to hydrolyze on NaY and AgY zeolites at room temperature, through cleavage of the P—S bond.[21] Decomposition of dimethyl methylphosphonate (DMMP) to methylphosphonate in sodium X zeolite (NaX) by nucleophilic zeolite reactions was reported,[22] together with the multiple effects of water on the nucleophilic substitution reaction.[23] However, the size limitation to diffusion into active supercage sites presented by the microporous NaX faujasite supercage was evident, and there is a strong need to enlarge the pore size from microporous to mesoporous to enhance adsorption. Meanwhile, the number of active sites [—Si-O(Na)-Al-] where the nucleophilic chemistry takes place

increases with Al content of the zeolite.[23] Therefore increasing zeolite Al content is also desirable.

In the present work, commercial NaX (Si/Al ~ 1.23), low-silica X zeolite (LSX, Si/Al ratio ~1.0),[24] and mesoporous NaX (MesoX), synthesized with an organic cationic polymer [poly-(diallyldimethylammonium chloride), PDADMAC] template with different molecular weights, were selected as the adsorbents. Trimethyl phosphate (TMP) was selected as a representative OP for adsorption into the different NaX zeolites. A stoichiometric amount of water was also introduced into the zeolites after the adsorption of OP in order to promote hydrolysis and possibly to recover the active sites. Textural characterization of the zeolites was performed by X-ray diffraction (XRD) and nitrogen adsorption analysis. The exposure of zeolites to TMP and the subsequent chemical reactions were examined with solid-state ^{31}P and ^{13}C cross-polarization (CP) and non-CP magic-angle spinning (MAS) nuclear magnetic resonance (NMR). The products and any residual reagent extracted from the exposed zeolite were examined with solution ^1H, ^{13}C, and ^{31}P NMR. An aqueous solution study of TMP base de-esterification and subsequent acidification in the Supporting Information serves to provide solution ^1H, ^{13}C, and ^{31}P NMR authentication for the zeolitic de-esterification in the zeolites. Nucleophilic substitution and subsequent hydrolysis reaction mechanisms are proposed, and the
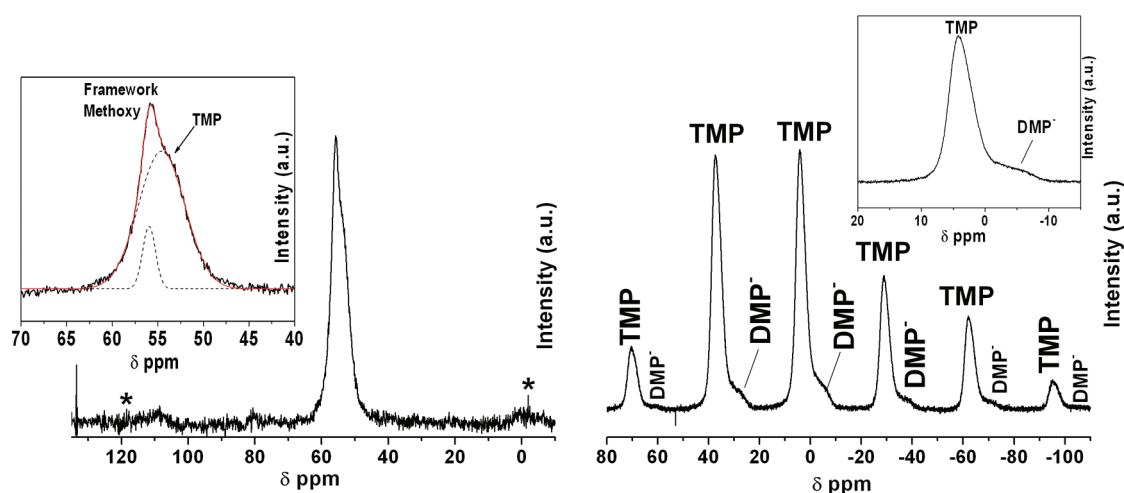
Figure 1. Solid-state ^{13}C (left) and ^{31}P (right) CP MAS NMR spectra of TMP-exposed NaX. (Inset) Simulation of peaks between 65 and 45 ppm (left), and peaks between 20 and −15 ppm (right).

Table 1. Assignments of NMR Spectra of TMP-Exposed NaX with and without Added Water and of Extracts from the Exposed NaX[a]

sample	^1H NMR peaks (ppm)	^{13}C NMR peaks (ppm)	^{31}P NMR peaks (ppm)
TMP-exposed NaX		54.0 (TMP), 56.0 (framework methoxy)	4.0[b] (TMP), −5.0[b] (DMP⁻)
TMP-exposed NaX with subsequent H_2O exposure		54.0 (TMP), 51.0 (DMHP and/or methanol)	4.0[b] (TMP), −5.0[b] (DMHP), −9.5[b] (MDHP and/or MHP⁻)
DMSO-d_6 extract of TMP-exposed NaX with subsequent H_2O exposure	3.7 (doublet, TMP), 3.2 (methanol CH₃), 3.3 (doublet, DMHP CH₃)	54.1 (doublet, TMP), 48.8 (methanol), 51.4 (DMHP)	3.6 (TMP), 2.2 (DMHP)
authentic CH_3OH in DMSO-d_6	3.2 (CH_3)	48.6 (CH_3)	
authentic TMP in DMSO-d_6	3.7 (doublet)	54.0 (doublet)	3.7
authentic DMHP in DMSO-d_6	3.6 (doublet)	52.9 (doublet)	2.0

[a] Assignments are made on the basis of given NMR chemical shifts of the authentic species in DMSO-d_6 solution, where available. [b] Solid-state ^{31}P NMR side-band structures are tabulated according to the maximum intensity side-band chemical shifts for comparisons between different solid samples; these will not necessarily agree with the liquid state ^{31}P chemical shifts, which effectively represent the weighted average of the side bands in the limit of zero spinning frequency.

TMP decomposition yields in various zeolites are compared for indications of possible improvements due to mesoporosity or higher Al content.

2. EXPERIMENTAL SECTION

NaX was purchased from Sigma—Aldrich. LSX was prepared according to the method of Su et al.[24] The preparation of MesoX was based on the method described by Xiao and co-workers.[25] PDADMAC polymer with two different molecular weight templates (<100 000 amu and 400 000—500 000 amu) were used. The two samples obtained were denoted MesoX-100 and MesoX-450, respectively.

TMP (from Sigma—Aldrich) was used as received. Deuterated dimethyl sulfoxide-d_6 (DMSO-d_6) was purchased from Cambridge Isotope Laboratories, Inc. The adsorption procedure is given in the Supporting Information. The amounts of TMP and water transferred to zeolites for hydrolysis were approximately 3 and 30 molecules per supercage of zeolites, respectively. Other experimental details on the instrumental methods, spectroscopic equipment and accuracy, and standards are presented in the Supporting Information.

3. RESULTS AND DISCUSSION

3.1. Structural Properties of the Zeolites. XRD patterns of the zeolites are shown in Figure 1S (Supporting Information). All the patterns exhibit structure characteristic of faujasite. Nitrogen adsorption experiments on the MesoX zeolites were also performed (see Figure 2S, Supporting Information). The nitrogen adsorption—desorption isotherms of all zeolites are of type I with a hysteresis loop of H4, and both samples show an obvious N_2 uptake below $P/P_0 \approx 0.02$. This is from the typical adsorption behavior of 1.3 nm supercages in NaX zeolites. A greater rate of uptake of N_2 by MesoX zeolites is observed than in commercial NaX (not shown) over the region $P/P_0 \approx 0.10-0.90$, the pressure region where the filling of the small micropores is essentially complete and the filling of the mesopores is taking place. In the pore size distribution curves a 40 Å feature is clearly observed, indicating a mesopore contribution from the organic template. Furthermore, an exceptionally broad pore size distribution band from 50 to 200 Å is also observed, similarly generated by the presence of organic template in the synthesis. The textural properties of the zeolites are summarized in Table 1S (Supporting Information). The micropore size of the zeolites is almost the same, indicating a similar micropore texture.

The Barrett–Joyner–Halenda (BJH) analysis shows a much higher mesopore contribution (20% for MesoX-100 and 14% for MesoX-450) than that in NaX (3.1%) or LSX (2.7%) (The mesopores in NaX and LSX may be due to the structural defects introduced during zeolite growth or degassing steps). This is also evidenced by the larger average pore size of MesoX zeolites (Table 1S, Supporting Information). According to the respective pore volumes, the zeolites are all predominantly microporous. But the MesoX zeolites have a significantly higher mesopore volume than NaX or LSX, consistent with the presence of organic polymer-templated mesopores.

3.2. TMP Adsorbed in Dry Zeolites. Solid-state ^{13}C and ^{31}P CP MAS NMR experiments were employed to identify the residual reagents and products in TMP-exposed zeolites, as shown in Figure 1.

Products, framework methoxy,[27] and unreacted TMP,[26] are assigned in Table 1 on the basis of literature refences,[26,27] authentic solution[26] (TMP) spectra, and a study of base hydrolysis of TMP in aqueous solution (Supporting Information). The leaving group anion from zeolite substitution into the TMP was not distinguished in the ^{13}C spectrum and may be overlapped by residual TMP in the broad feature between 65 and 45 ppm. Figure 1 (right) shows more clearly two different phosphorus-containing species, TMP and dimethyl phosphate (DMP$^-$) product, which is not distinguished in the ^{13}C spectrum. DMP$^-$ anion is assigned on the basis of TMP base hydrolysis products in aqueous solution (Supporting Information) since authentic DMP$^-$ salts are not commercially available. The solid-state NMR spectra of TMP-exposed LSX and MesoX are similar to those of NaX and are not shown.

In order to compare the chemical reactivity of different zeolites, the integrated intensity ratio (R) between DMP$^-$ ion and TMP in solid-state ^{31}P NMR (non-CP) spectra was also determined and used to calculate the yield (Y), according to $Y = R/(R + 1)$. The yields of TMP shown in Table 2 in the various forms of NaX are all identical within experimental error.

Table 2. Product Yields Determined from Integrated Intensity Ratios of Residual Reagent and Product Peaks of Solid-State ^{31}P NMR Spectra without CP in TMP-Exposed Zeolites

	commercial NaX	LSX	MesoX–100	MesoX–450
R (TMP)	0.45 ± 0.10	0.47 ± 0.02	0.48 ± 0.02	0.51 ± 0.02
Y (TMP, %)	31.0 ± 0.9	32.9 ± 1.2	32.4 ± 1.2	33.8 ± 1.2

Extraction of TMP-exposed zeolites with organic solvents was performed and further investigation of the solution NMR spectra of the extract was done. But no new feature other than those of authentic TMP was observed. The decomposition product, DMP$^-$ ion, might be strongly attracted to the Na$^+$ of the zeolite and therefore difficult to extract. The framework methoxy is covalently bonded to the zeolite framework.

3.3. TMP Adsorbed in Zeolites and Subsequent Addition of Stoichiometric Water. *3.3.1. Solid-State NMR Spectra of TMP-Exposed Zeolite with Water Addition.* Shown in Figure 2 are the solid-state ^{13}C (A) and ^{31}P (B) CP MAS NMR spectra of TMP-exposed NaX, subsequently exposed to 30 molecules of water per supercage. Water is hydrolyzing the decomposition products of TMP in the zeolites. TMP[26] and products, framework methoxy,[27] methanol (MeOH),[28] DMP$^-$, and dimethyl hydrogen phosphate (DMHP) are assigned, as shown in Table 1, on the basis of literature references,[26,28] authentic solution (TMP, MeOH, DMHP) spectra, and a study of base hydrolysis and acidification products of TMP in aqueous solution (Supporting Information). Methanol is the hydrolysis product of framework methoxy. The hydrolysis product of DMP$^-$ ion, DMHP, is not clearly distinguishable from methanol in the ^{13}C spectrum. In the ^{31}P spectrum, DMHP was also not distinguishable from DMP$^-$ (Supporting Information), but MeOH and DMHP were successfully found in the solvent extract of this sample (to be described in section 3.3.2).

The observation of a third, complex peak, comprising two features at −9.0 and −10.0 ppm, is unexpected on the basis of a single de-esterification of TMP. These unexpected features can reasonably be assumed to be the products of chemistry between the relatively mobile DMHP molecule (compared to less mobile DMP$^-$ ion in experiments without water) and remaining active sites in zeolite. The products would be monomethyl hydrogen phosphate (MHP$^-$) ion and its hydrolysis product, monomethyl dihydrogen phosphate (MDHP). (See Supporting Information for an explanation why preparation of authentic samples of these species by base de-esterification was not possible in solution.) Authentic MHP$^-$ salts and MDHP are not commercially available. Successive zeolite de-esterification has been observed in DMMP.[23] From the decontamination perspective, it should be noted that this proposed step removes the second methoxy group of TMP. However, there was no indication of the removal of the third methoxy group, since the likely narrow peak of mobile phosphoric acid did not appear to be present near its zero chemical shift reference position. In contrast, the hydrolysis of TMP in water
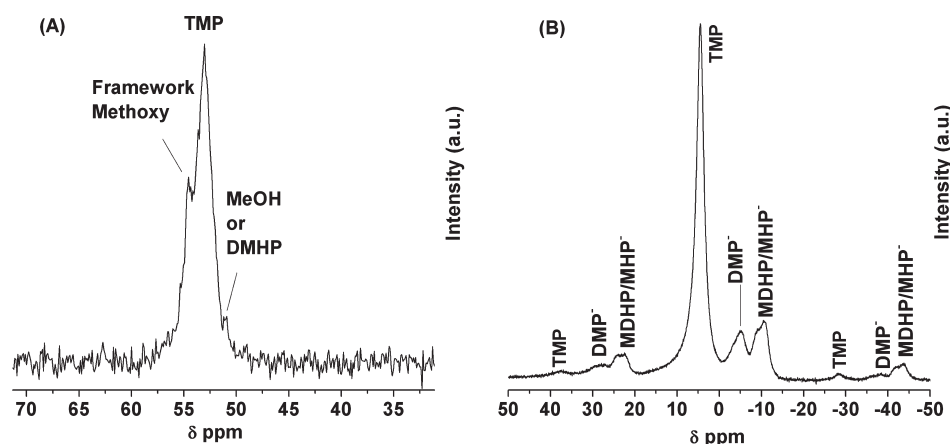

Figure 2. Solid-state ^{13}C (A) and ^{31}P (B) CP MAS NMR spectra of TMP-exposed NaX with addition of 30 molecules of water per supercage.

cannot go beyond the first methoxy group, even in strongly basic NaOH solution (Supporting Information). So the probable observation of MDHP and MHP[−] ion indicates the excellent potential NaX zeolite may have in the decontamination of OPs, insofar as the toxicity of the OP becomes less with each successive ester group removal. Generally the addition of limited water, which is often being associated with the poisoning of zeolites, generates a
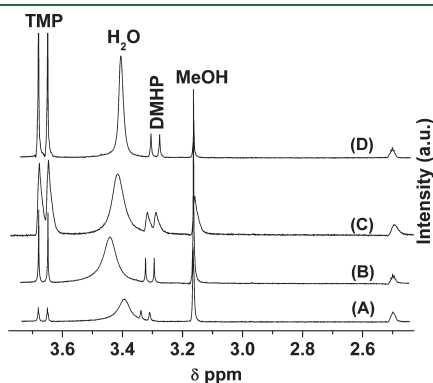

Figure 3. Solution ^{1}H NMR spectra of DMSO-d_6 extract of TMP-exposed zeolites to which 30 molecules per supercage of water were subsequently added. (A) Commercial NaX; (B) LSX; (C) MesoX-100; (D) MesoX-450. The peak around 2.5 ppm is from the isotopic impurity.

DMHP molecule by hydrolysis of the immobile DMP[−] ion. The DMHP molecule is mobile enough to migrate to another active zeolite site, in turn promoting the removal of the second methoxy group of TMP.

3.3.2. Solution NMR Spectra of Extracts of TMP-Exposed Zeolites with Water Addition. The hydrolysis products of TMP-exposed zeolites after water addition were extracted by DMSO-d_6. The extracts were examined by solution ^{1}H, ^{13}C, and ^{31}P NMR spectra and the results are presented in Figures 3 and 4. TMP[26] and products, MeOH[28] and DMHP, are assigned, as shown in Table 1, on the basis of literature references,[26,28] authentic solution (TMP, MeOH, DMHP) spectra, and a study of TMP and its base hydrolysis and acidification products in aqueous solution (Supporting Information). The broad peak at around 3.4 ppm in Figure 3 A is assigned to ^{1}H in unconsumed water. It shifts to lower fields with greater intensities in panels B—D, which is due to the presence of different amounts of water extracted.[23] But the third de-estification products of MHP[−] and MDHP were not present in the solution NMR, which might be due to their tiny amounts. The species found in the extract spectra and their assignments further support the identification of the species found in the solid samples in sections 3.2 and 3.3.1 and the assignment of their NMR spectra.

3.4. Mechanism. Based on the solid-state ^{31}P and ^{13}C NMR results on TMP-exposed zeolites before and after water addition and the solution NMR results on the extracts, a proposed
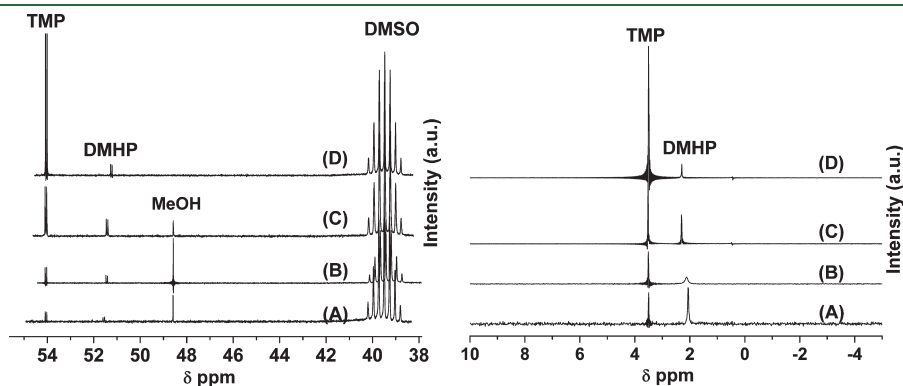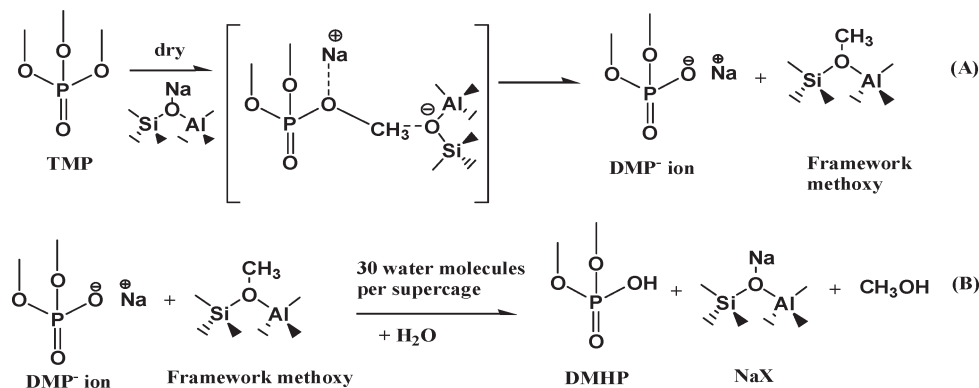

Figure 4. Solution ^{13}C (left) and ^{31}P (right) NMR spectra of DMSO extracts of TMP- exposed (A) NaX, (B) LSX, (C) MesoX-100, and (D) MesoX-450 to which 30 molecules of water per zeolite supercage were subsequently added.

Scheme 1. Proposed Reaction Mechanism of TMP (A) Adsorbed into Dry Zeolite and (B) with Subsequent Addition of Stoichiometric Amount of Water

mechanism for the formation of DMP$^-$ ion and DMHP is shown in Scheme 1.

When TMP is absorbed into the zeolite, the nucleophilic zeolitic oxygen interacts with a carbon of one of the methyl groups and the Na$^+$ counterion interacts with the methyl ester oxygen atom. The interaction between Na$^+$ counterion and oxygen atom polarizes the ester C—O bond, leading to a methyl elimination reaction.[23] The resulting dimethyl phosphate (DMP$^-$) ion is stabilized by zeolitic Na$^+$ cations released in the formation of framework methoxy zeolite sites, which have been observed and identified in the ^{13}C NMR solid-state spectrum (Figure 1).

After addition of water, as depicted in Scheme 1 B, the DMP$^-$ ion is hydrolyzed and the Na$^+$ cation is replaced by an H$^+$. A stable molecule of dimethyl hydrogen phosphate (DMHP) is formed. The leaving OH$^-$ from the hydrolyzing water ion hydrolyzes the framework methoxy, leading to methanol formation. The Na$^+$ released from NaDMP hydrolysis replaces the methyl carbocation released from framework methoxy hydrolysis. This hypothesis is confirmed by the observation of methanol in both extract ^{1}H and ^{13}C NMR spectra of TMP-exposed zeolites after water addition, as shown in Figures 3 and 4. Through de-esterification and hydrolysis of the first methoxy group by zeolite, TMP is decomposed to DHMP. The additional peaks observed under hydrolyzing conditions in Figure 2B lead to the explanation that DHMP can react further with remaining active sites in the zeolite. Reaction leads to de-esterification of the second methoxy group. Accordingly, the new features are tentatively assigned to the products of the second methoxy group de-esterification, that is, MHP$^-$ ion and hydrolysis product MDHP. This would indicate the capability of NaX with limited adsorbed water to decontaminate OPs at room temperature in a way that is more complete chemically and more environmentally friendly than strongly basic solutions or other solid catalysts that require heat.

Finally, it is disappointing that manipulation of the zeolite porosity and increasing the Al content do not substantially increase the yields. Evidently, the substantial regions of NaX crystallinity in all of the samples serve to limit the yields because of slow diffusion in these microporous regions, no matter the mesoporosity or Al content.

ASSOCIATED CONTENT

S   Supporting Information.   Eleven figures, four tables, and additional text, describing a parallel study of tri-*n*-propyl phosphate (TPP), which gives results essentially identical to the TMP results, supporting their generality; a study of base-catalyzed de-esterification of TMP and subsequent acidifction of the products in water solution, which serves to provide solution ^{1}H, ^{13}C, and ^{31}P NMR authentication for zeolite de-esterification; and additional experimental details. This material is available free of charge via the Internet at http://pubs.acs.org.

AUTHOR INFORMATION

Corresponding Author
*Tel: +1 6077772769; fax: +1 6077774478; e-mail: qmeng@ binghamton.edu.

ACKNOWLEDGMENT

REFERENCES

(1) Banks, K. E.; Hunter, D. H.; Wachal, D. J. Chlorpyrifos in surface waters before and after a federally mandated ban. *Environ. Int.* **2005**, *31*, 351–356.

(2) Yang, Y. C.; Baker, J. A.; Ward, J. R. Decontamination of chemical warfare agents. *Chem. Rev.* **1992**, *92*, 1729–1743.

(3) Wilcox, D. E. Binuclear metallohydrolases. *Chem. Rev.* **1996**, *96*, 2435–2458.

(4) Vlyssides, A.; Barampouti, E. M.; Mai, S.; Arapoglou, D.; Kotronarou, A. Degradation of methylparathion in aqueous solution by electrochemical oxidation. *Environ. Sci. Technol.* **2004**, *38*, 6125–6131.

(5) Kolinko, P. A.; Kozlov, D. V. Photocatalytic oxidation of tabun stimulant-diethyl cyanophosphate: FTIR in situ investigation. *Environ. Sci. Technol.* **2008**, *42*, 4350–4355.

(6) Kim, D. B.; Gweon, B.; Moon, S. Y.; Choe, W. Decontamination of the chemical warfare agent stimulant dimethyl methylphosphonate by means of large-area low-temperature atmospheric pressure plasma. *Curr. Appl. Phys.* **2009**, *9*, 1093–1096.

(7) Zuo, G. M.; Cheng, Z. X.; Li, G. W.; Shi, W. P.; Miao, T. Study on photolytic and photocatalytic decontamination of air polluted by chemical warfare agents (CWAs). *Chem. Eng. J.* **2007**, *128*, 135–140.

(8) Fei, X; Sun, G. Oxidative degradation of organophosphorous pesticides by N-halamine fabrics. *Ind. Eng. Chem. Res.* **2009**, *48*, 5604–5609.

(9) Dai, K.; Peng, T. Y.; Chen, H.; Liu, J.; Zan, L. Photocatalytic degradation of commercial phoxim over La-doped TiO$_2$ nanoparticles in aqueous suspension. *Environ. Sci. Technol.* **2009**, *43*, 1540–1545.

(10) Wagner, G. W.; Bartram, P. W.; Koper, O; Klabunde, K. J. Reactions of VX, GD, and HD with nanosize MgO. *J. Phys. Chem. B* **1999**, *103*, 3225–3228.

(11) Wagner, G. W.; Procell, L. R.; O'Connor, R. J.; Munavalli, S.; Carnes, C. L.; Kapoor, P. N.; Klabunde, K. J. Reactions of VX, GB, GD, and HD with nanosize Al$_2$O$_3$. Formation of aluminophosphonates. *J. Am. Chem. Soc.* **2001**, *123*, 1636–1644.

(12) Wagner, G. W.; Procell, L. R.; Munavalli, S. ^{27}Al, ^{47,49}Ti, ^{31}P, and ^{13}C MAS NMR study of VX, GD, and HD reactions with nanosize Al$_2$O$_3$, conventional Al$_2$O$_3$ and TiO$_2$, and aluminum and titanium metal. *J. Phys. Chem. C* **2007**, *111*, 17564–17569.

(13) Mahato, T. H.; Prasad, G. K.; Singh, B.; Acharya, J.; Srivastava, A. R.; Vijayaraghavan, R. Nanocrystalline zinc oxide for the decontamination of sarin. *J. Hazard. Mater.* **2009**, *165*, 928–932.

(14) Panayotov, D. A.; Morris, J. R. Catalytic degradation of a chemical warfare agent stimulant: Reaction mechanisms on TiO$_2$-supported Au nanoparticles. *J. Phys. Chem. C* **2008**, *112*, 7496–7502.

(15) Columbus, I.; Waysbort, D.; Shmueli, L.; Nir, I.; Kaplan, D. Decomposition of adsorbed VX on activated carbons studied by ^{31}P MAS NMR. *Environ. Sci. Technol.* **2006**, *40*, 3952–3958.

(16) Bromberg, L.; Schreuder-Gibson, H.; Creasy, W. R.; McGarvey, D. J.; Fry, R. A.; Hatton, T. A. Degradation of chemical warfare agents by reactive polymers. *Ind. Eng. Chem. Res.* **2009**, *48*, 1650–1659.

(17) Gomes, D. E. B.; Lins, R. D.; Pascutti, P. G.; Lei, C. H.; Soares, T. A. The role of nonbonded interactions in the conformational dynamics of organophosphorous hydrolase adsorbed onto functionalized mesoporous silica surfaces. *J. Phys. Chem. B* **2010**, *114*, 531–540.

(18) Seger, M. R.; Maciel, G. E. NMR investigation of the behavior of an organothiophosphate pesticide, chlorpyrifos, sorbed on montmorillonite clays. *Environ. Sci. Technol.* **2006**, *40*, 797–802.

(19) Seger, M. R.; Maciel, G. E. NMR investigation of the behavior of an organothiophosphate pesticide, chlorpyrifos, sorbed on soil components. *Environ. Sci. Technol.* **2006**, *40*, 791–796.

(20) Knagge, K.; Johnson, M.; Grassian, V. H.; Larsen, S. C. Adsorption and thermal reaction of DMMP in nanocrystalline NaY. *Langmuir* **2006**, *22*, 11077–11084.

(21) Wagner, G. W.; Bartram, P. W. Reaction of VX, HD, and their stimulants with NaY and AgY zeolites. Desulfurization of VX on AgY. *Langmuir* **1999**, *15*, 8113–8118.

(22) Yang, S. W.; Doetschman, D. C.; Schulte, J. T.; Sambur, J. B.; Kanyi, C. W.; Fox, J. D.; Kowenje, C. O.; Jones, B. R.; Sherma, N. D. Sodium X-type faujasite zeolite decomposition of dimethyl methylphosphonate (DMMP) to methylphosphonate: Nucleophilic zeolite reactions I. *Microporous Mesoporous Mater.* **2006**, *92*, 56–60.

(23) Sambur, J. B.; Doetschman, D. C.; Yang, S. W.; Schulte, J. T.; Jones, B. R.; DeCoste, J. B. Multiple effects of the presence of water on the nucleophilic substitution reactions of NaX faujasite zeolite with dimethyl methylphosphonate (DMMP). *Microporous Mesoporous Mater.* **2008**, *112*, 116–124.

(24) Su, B. L.; Roussel, M.; Vause, K.; Yang, X. Y.; Gilles, F.; Shi, L.; Leonova, E.; Edén, M.; Zou, X. Organic group-bridged hybrid materials with a faujasite X zeolite structure (ZOF-X). *Microporous Mesoporous Mater.* **2007**, *105*, 49–57.

(25) Liu, S. Z.; Cao, X. J.; Li, L. S.; Li, C. J.; Ji, Y. Y.; Xiao, F. S. Preformed zeolite precursor route for synthesis of mesoporous X zeolite. *Colloids Surf., A* **2008**, *318*, 269–274.

(26) Streck, R.; Barnes, A. J. Solvent effects on infrared, ^{13}C and ^{31}P NMR spectra of trimethyl phosphate: Part 1. Single solvent systems. *Spectrochim. Acta A* **1999**, *55*, 1049–1057.

(27) Bosáček, V.; Ernst, H.; Freude, D; Mildner, T. Surface methoxy groups in zeolites studied by multinuclear MAS NMR spectroscopy. *Zeolites* **1997**, *18*, 196–199.

(28) Gottlieb, H. E.; Kotlyar, V.; Nudelman, A. NMR chemical shifts of common laboratory solvents as trace impurities. *J. Org. Chem.* **1997**, *62*, 7512.